2008 IEEE International Conference on
Robotics and Automation
Pasadena, CA, USA, May 19-23, 2008

Optical Fiber Sensor for Soft Tissue Investigation during Minimally Invasive Surgery

Pinyo Puangmali, Hongbin Liu, Kaspar Althoefer, *Member, IEEE*, Lakmal D. Seneviratne, *Member, IEEE*

***Abstract*—This paper describes the preliminary design and construction of an optical fiber sensor which has been developed for evaluating the feasibility of using an optical-based force sensing methodology to investigate mechanical soft tissue properties during minimally invasive surgery. This sensor applies a novel reflective light intensity modulation scheme using bent-tip optical fibers and a reflector to measure mechanical response of the soft tissue when it interacts with the sensor. By adopting such optical fibers to detect minute deflection of a flexible cylindrical structure at the reflective edge of the reflector, good sensitivity for the force detection can be obtained. The prototype described in this document has demonstrated that it can detect the tissue interaction forces in the axial direction and identify variations in tissue stiffness. The maximum force range that can be detected by the sensor is 3 N. The measurement resolution is 0.02 N.**

I. Introduction

MINIMALLY invasive surgery (MIS) is described as a surgical operation that the surgeon performs through small incisions. This surgical technique is clearly becoming the preferred approach compared to conventional open surgery since it offers various advantages including the reduction of intraoperative blood loss, tissue trauma, risk of post operative infection, pain experienced by the patient, and recovery time. However, because the MIS operating field is not directly accessed, surgeons face many difficulties in performing their operations through small "key holes" with limited vision. The motion of surgical instruments is also considerably constrained by the fulcrum at the instrument insertion port (trocar port) allowing only movement along four possible degrees of freedom (insertion, pitch, yaw, and roll). Moreover, the capability of obtaining force and tactile information, referred to as haptic perception when the tissue interacts with the surgical instrument, is greatly impaired by friction between the instrument shaft and the insertion port. This prevents palpation information from being delivered effectively to the surgeon, and thus, reduces the ability to examine tissue properties and abnormalities during the surgery.

To overcome the problems due to the lack of force and tactile information, various sensing techniques which apply either a direct sensing scheme using a force sensor [1]–[3] or an indirect force sensing scheme using a disturbance observer [4] have been adopted. The size and the complexity of the force sensing devices depend on the number of force measurement axes required for particular surgical purposes. Even though the force can be detected by those sensing methods, there still are limitations in accuracy, repeatability, measurement range, and sterilizability.

Fig. 1. Force sensitive wheeled probe.

Recently, research on soft tissue property identification for MIS has been conducted aiming to provide a surgeon with the ability to palpate soft tissue organs within the human body and identify properties of organic tissues. A force sensitive wheeled probe, which can be used to perform both static and rolling indentation, has then been proposed [5]. Compared to traditional static indentation probes, the wheeled probe allows the surgeon to investigate a large tissue area in much shorter time. The wheeled probe instrumented with a commercial force sensor has already been tested and used to localize miniature buried masses *ex-vivo* [5]. The wheeled probe integrated with a miniature force sensitive device shown in Fig. 1 is to be used for conducting *in-vivo* tissue property identification and abnormal underlying mass localization. It is expected that the force sensitive wheeled probe could be a useful tool that aids surgeons in carrying out a variety of minimally invasive surgical operations more effectively. These could include finding blockage of an artery during a coronary artery bypass grafting procedure in minimally invasive cardiac surgery or identifying areas of tumourous tissue for prostatectomy, hysterectomy, cholecystectomy, cystectomy, and naphrectomy. This paper introduces a laboratory prototype of such an instrument.

Manuscript received September 12, 2007.

P. Puangmali, H. Liu, K. Althoefer, and L. D. Seneviratne are with King's College London, Department of Mechanical Engineering, Strand, London, WC2R 2LS, UK (e-mail: pinyo.puangmali@kcl.ac.uk, hongbin.liu@kcl.ac.uk, k.althoefer@kcl.ac.uk, lakmal.seneviratne@kcl.ac.uk).

Based on an optical fiber sensing scheme, the force exerted on the sensor as a result of the interaction between the sensor tip and the tissue can be measured by monitoring a change of the intensity of the light traveling through the optical fibers.

II. Device Design

To perform surgery in a minimally invasive manner, a surgeon usually inserts straight long tools known as either endoscopic or laparoscopic instruments through incisions of approximately 3-12 mm diameter [6]. This is a very delicate operation that requires effective instruments and well trained skills from the surgeon to overcome the loss of intuitive feel during the surgical operation. One way to augment effectiveness of MIS is to integrate a force sensing element with a surgical instrument allowing the tissue interaction force information to be captured and delivered to the surgeon. However, this cannot be easily implemented due to various design and usage constraints. Before any practical force sensing solution can be introduced to keyhole surgery, it is important that a number of requirements are considered:

- The sensing components should be sensitive and located closely to the instrument tip such that the tissue interaction force exerted on it can be detected effectively.
- The size of the sensor must not exceed the size of the standard instrument insertion port (trocar port) through which it is to be inserted during surgery.
- The sensor should be completely sealed to prevent body liquids affecting internal sensing elements.
- The sensor should be sterilizable with a standard sterilization protocol.

Optical-based sensors are well suited for this application since they offer several advantages over conventional sensors like strain gauge load cells. These include small size, high sensitivity, fast response time, immunity to electromagnetic interference, and completely electrical isolation from other electronics.

An early attempt of using the optical sensing strategy for force detection was proposed by Hirose and Yoneda [7]. Subsequently, it has been applied in various applications including robotic surgery. Applying an optical sensing scheme is an alternative way to measure and transfer force information. Instead of using electrical wires to carry electrical signals, fiber optic cables can be used as a medium to carry force information from a sensing field to opto-electronic equipment located remotely. Optical fiber force sensing devices have found their applications in MIS as reported in [1], [8] for the development of an MIS instrument shaft sensor and a force sensitive grasping instrument. Both applied similar light modulation mechanisms using optical fibers and a reflector to perform force measurements by detecting the distance between its reflective surface and a fiber tip. The sensor presented in this paper was constructed based on a different reflective modulation mechanism using bent-tip optical fibers and a reflector to detect forces by monitoring the shifting of the reflector edge.

A. Measurement Principle

The underlying principle of the sensor described in this paper is based on the configuration that measures small linear translational displacements between the bent-tip optical fibers and the edge of a reflector. In this sensing configuration (see Fig. 2), a pair of symmetrically identical bent-tip fibers is used. One is the transmitting fiber which is used for guiding the light from the light source to the reflector. Another is the receiving fiber which is used for collecting the light reflected from the reflector and delivering it to the photodetector. Both fibers are affixed to a rigid structure whereas the reflector is placed on a flexible structure called flexure. A force applied to the flexure results in a bending moment deforming the structure and causing an offset between the fiber tips and the edge of the reflector. This, thus, varies the light reflected to the receiving fiber leading to changes of the light intensity measured at the detector (Note that due to the flexure deformation, the reflector may also tilt and the distance between the fiber tips and the reflective surface may also slightly change. However, those do not significantly affect the light intensity when compared to the shift of the reflector edge in this structure). By converting the light intensity into an electrical signal and further processing it through a photo-electronic circuit, the magnitude of the force applied can be determined and read out by a computer or monitored by an oscilloscope.

Fig. 3 shows the geometry of the bent-tip optical fibers sensing configuration for force detection. The transmitting fiber and the receiving fiber are placed at an angle α with reference to each other. The fiber tips are separated by a distance of a. The reflector is located below at a distance of h from the fiber tips. Since a flat reflector is applied, it can be inferred that the transmitting fiber seen by the receiving fiber is virtually located beneath the reflective surface. Such

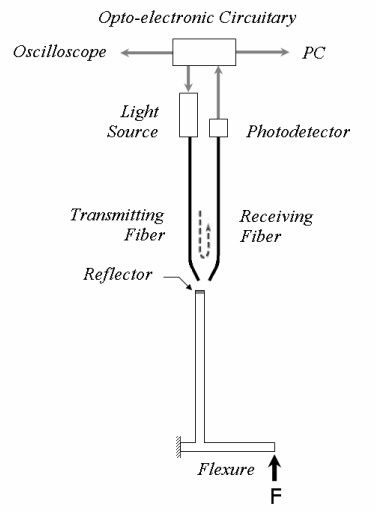

Fig. 2. Schematic diagram of the proposed optical fiber sensor.

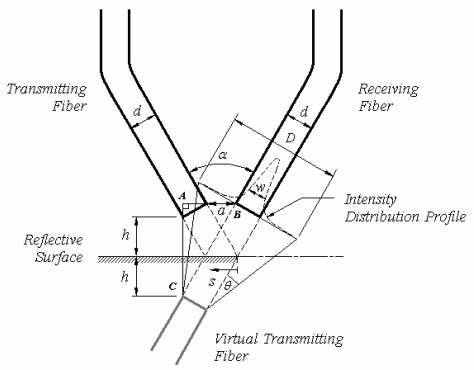

Fig. 3. Geometry of the bent-tip optical fiber sensing configuration.

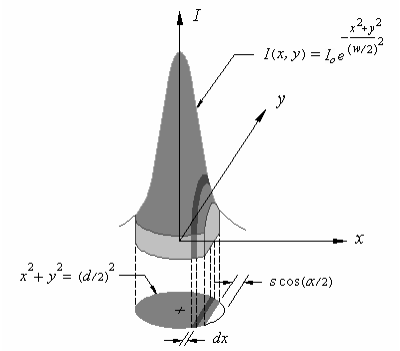

Fig. 4. Model of the light flux collected by the receiving fiber; the intensity distribution profile is bounded by the effective light transmitting area seen by the receiving fiber.

a virtual transmitting fiber appears to project a conical light beam to the receiving fiber.

In this sensing configuration, the distance between the receiving fiber and the virtual transmitting fiber $\overline{BC}$ is found to be

$$\overline{BC}=\frac{2h}{\cos(\alpha/2)}+\frac{d}{\cos(\alpha/2)}\sin(\alpha/2). \tag{1}$$

The diameter of the projected light circle is

$$D=d+2\overline{BC}\tan\theta=d+2\left(\frac{2h}{\cos(\alpha/2)}+\frac{d}{\cos(\alpha/2)}\sin(\alpha/2)\right)\tan\theta, \tag{2}$$

where θ represents the radiation angle of the optical fiber. The relation between h and a can also be defined by considering the triangle ΔABC where

$$\begin{aligned} a&=\overline{BC}\sin(\frac{\alpha}{2})-d\cos(\frac{\alpha}{2}) \\ &=\left(\frac{2h}{\cos(\alpha/2)}+\frac{d}{\cos(\alpha/2)}\sin(\alpha/2)\right)\sin(\frac{\alpha}{2})-d\cos(\frac{\alpha}{2}) \end{aligned} \tag{3}$$

and

$$h=\frac{a\cos(\alpha/2)+d\cos^2(\alpha/2)-d\sin^2(\alpha/2)}{2\sin(\alpha/2)}. \tag{4}$$

The approximate intensity distribution profile of the projected light beam is assumed to be of a Gaussian form which is expressed in polar coordinates as

$$I(r)=I_o e^{-\frac{r^2}{(w/2)^2}}, \tag{5}$$

where r is the radial distance of the projected light beam, I_o is the maximal intensity of the projected light beam, and w is the Gaussian width at $1/e$ of the peak. In a Cartesian coordinate, the intensity distribution profile is expressed as

$$I(x,y)=I_o e^{-\frac{x^2+y^2}{(w/2)^2}}. \tag{6}$$

The total light flux emitted to the end face plane of the receiving fiber ϕ_t are calculated by

$$\phi_t=\int_0^{D/2} I(r)\cdot 2\pi r dr, \tag{7}$$

where D is the maximal diameter of the projected area on the receiving fiber end face plane. Since the light flux coupled into the receiving fiber ϕ_r is limited to the overlap area between the circular pattern of the projected area and the cross-sectional area of the receiving fiber which is usually smaller, the light flux collected by the receiving fiber is therefore bounded by the size of the fiber. With respect to this, the maximal possible collected light flux can be expressed as

$$\phi_{r,\max}=\int_0^{d/2} I_o e^{-\frac{r^2}{(w/2)^2}}\cdot 2\pi r dr=\frac{\pi}{4}w^2 I_o(1-e^{-\frac{d^2}{w^2}}). \tag{8}$$

Depending on the amount of the collected light flux, the maximal output of the light detector is

$$U_{\max}=k_v\sigma_r\phi_{r,\max}=\frac{\pi}{4}k_v\sigma_r w^2 I_o(1-e^{-\frac{d^2}{w^2}}), \tag{9}$$

where k_v is the transforming factor of the light detector that converts the total light flux into electrical output, and σ_r represents the losses in the receiving fiber including the losses due to bending. In Fig. 3, a reflective surface is also demonstrated. It lies at the position that allows highest light flux to be coupled into the receiving fiber. When the reflector shifts to the left hand side, a part of the transmitted light will not be reflected and, hence, only a portion of the light is reflected to the receiving fiber. This causes less light flux to be collected by the receiving fiber, and thus, the light intensity to be reduced.

Fig. 4 shows a model of the collected light flux which is bounded by the effective light transmitting area of the transmitting fiber seen by the receiving fiber. If the reflector shifts aside by a distance of s, the straight edge of the effective light transmitting area will be shifted by a distance of $s\cos(\alpha/2)$. With regard to this, the variation of the light flux collected by the receiving fiber can be approximated as

$$\phi_r=2I_o\int_{-\frac{d}{2}}^{\frac{d}{2}-s\cos\frac{\alpha}{2}}\int_0^{\sqrt{(\frac{d}{2})^2-x^2}} e^{-\frac{x^2+y^2}{(w/2)^2}}dydx \tag{10}$$

and the output of the light detector is

$$U = k_v \sigma_r \phi_r = 2k_v \sigma_r I_o \int_{-\frac{d}{2}}^{\frac{d}{2}-s\cos\frac{\alpha}{2}} \int_{0}^{\sqrt{(\frac{d}{2})^2 - x^2}} e^{-\frac{x^2+y^2}{(w/2)^2}} dydx. \quad (11)$$

The ratio between the output of the light detector and its maximal possible value defines the normalized output

$$\frac{U}{U_{\max}} = \frac{8}{\pi w^2 (1 - e^{-\frac{d^2}{w^2}})} \int_{-\frac{d}{2}}^{\frac{d}{2}-s\cos\frac{\alpha}{2}} \int_{0}^{\sqrt{(\frac{d}{2})^2 - x^2}} e^{-\frac{x^2+y^2}{(w/2)^2}} dydx. \quad (12)$$

Eq. (12) is the new nonlinear mathematical model proposed to describe the sensing characteristics of this light intensity modulation configuration. To verify such sensing characteristics experimentally, a set of experiments were performed with a pair of polymer optical fibers, which have a core diameter of 1 mm, a length of 80 cm, the reflective index of 1.49 and an acceptance angle of +/-32°. The fiber tips were placed in front of each others separated by a distance of 1 mm. A 1.25-watt high-intensity light emitting diode (LED) and a photodiode (Siemens SFH 2030) were coupled to the transmitting and receiving fiber respectively. A flat rectangular reflector was located at a distance between the fiber tips and its reflective surface as defined by (4). Fig. 5 shows the comparison of simulated and measured responses of the sensing configuration which is composed of a fiber pair placed at angles α = 30°, 60°, and 90°. In this experiment, the Gaussian widths were set such that they could provide good matches between the simulated curves and the experimental data (well-defined values could compensate for the model errors due to, for instance, the limited reflectivity of the reflector, the imperfection of the fiber end faces, the mechanical misalignment between the fiber cores, and the nonlinearity of the photodiode). For the angles α = 30°, 60°, and 90°, the corresponding values were w = 0.55 mm, 0.59 mm, and 0.63 mm. As can be seen in Fig. 5, the simulated curves obtained from (12) can approximate the measured responses obtained from the experiment fairly accurately. The root mean square (RMS) errors are 4.7%, 3.5%, and 2.5% for the configuration with angles α = 30°, 60°, and 90° respectively.

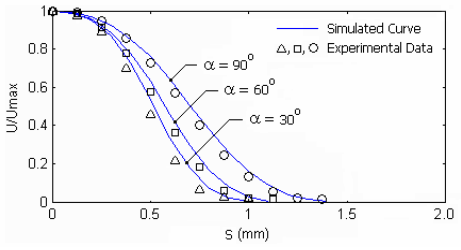

Fig. 5. Simulated and measured responses of the sensing configuration.

B. Flexible Structure

Similar to many force sensing devices, the sensitivity of the sensor described in this paper much depends on the flexibility of its structure. Because the sensing principle is based on the measurement of the structural deformation, there is trade-off between the rigidity of the sensor structure and the sensitivity of the measurement. As being a part of the instrument shaft, high stiffness characteristic of the sensor structure is substantial for sustaining distal instruments including the distal wheel and its support under loaded conditions. Unfortunately, a stiff structure tends to provide low measurement sensitivity. To obtain good measurement sensitivity whilst maintaining high stiffness characteristics of the structure, a flexure made of a hollow cylindrical shaft which has a partial cut was employed with an internal straight long bar mounted along its central axis. Such a long bar offers an amplifying effect that allows the deflection of the flexure to be enlarged at its tip, where the reflector is located and its edge is to be detected (see Fig. 6). When the tissue interaction force is exerted on the sensor, the sensor structure will be deformed allowing the interaction between the sensor and the tissue to be detected. Because the length of the bar and the size of the partial cut greatly influence the measurement sensitivity of the sensor, they were therefore carefully optimized such that good measurement sensitivity can be obtained without excessive violation to structural rigidity.

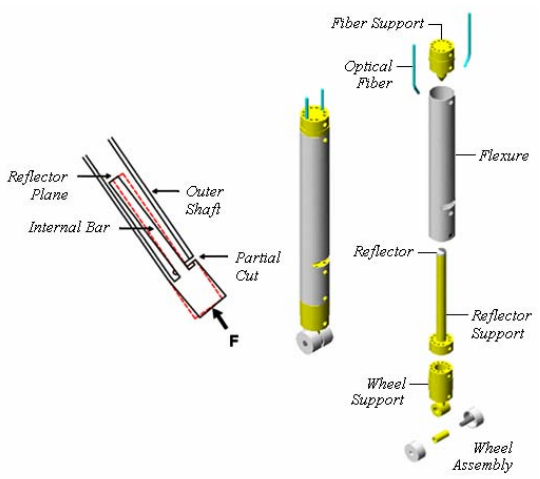

Fig. 6. Exaggerated deformation diagram and sensor components.

C. Prototype

To realize the design, the first prototype shown in Fig. 6 was constructed. The hollow flexure was made from a chromium-plated brass tube. A pair of identical bent-tip fibers was attached with a central cone-shape support. One is for projecting the light to another through a 4-mm-diameter semi-circular reflector placed on its straight long support. The angle α between the fiber tips was set to be 60°. This angle was selected because it offers good sensing ability without too much bending the tips of the fibers. In addition, the wheel (composed of two 8-mm-diameter wheel parts) and its support were also integrated at the distal end of the sensor. The wheel has an overall width of 9 mm. In this prototype, the reflector is made of a polished aluminum sheet.

As with the test system, the optical fibers employed are 1-mm-diameter plastic fibers, which have the reflective index of 1.49 and an acceptance angle of +/-32°. The light source used to project the light to the fibers is a 1.25-watt high-intensity LED. The light detector is a photodiode (Siemens SFH 2030). The output of the photodiode is filtered and amplified to an output voltage range of 0-3 V. The whole sensor has a diameter of 10 mm and a length of 92.4 mm.

III. Experimental Results

A. Loading and Unloading Tests

To verify sensing characteristics, the sensor was initially mounted with a long shaft and held upright. It was then loaded with a set of weights of each 9.5 g up to a maximal load of 3 N, and then the load was removed. The responses of the sensor under loading and unloading conditions were recorded and plotted as shown in Fig. 7 (a). Similar loading and unloading test was also carried out with a set of weights of each 3.56 g when the sensor was held horizontally. The responses of the sensor under lateral loading and unloading conditions when it was held such that it provided highest sensitivity are shown in Fig. 7 (b).

As shown in Fig. 7, the sensor exhibited very low hysteresis. It provides good sensitivity and repeatability for the detection of forces both in axial and particular lateral directions. The sensitivity for the force detection in the axial direction is nearly constant at 0.45 V/N but the sensitivity for the force detection in lateral directions varies from 0.13-3.19 V/N depending on the radial direction of the force applied (The lateral force sensitivity is lowest in the direction parallel to the straight reflective edge of the reflector and highest in the direction perpendicular to it). When the sensor was equipped with the wheel, the rolling direction of the wheel was set to be parallel to the direction that provides lowest sensitivity in the lateral direction. This decouples the effects of the axial and lateral forces, and also allows the applied forces in the axial direction to be detected in a wide range during rolling indentation actions. In this prototype, the amplitude of sensor noise was found to be 10 mV peak-to-peak. This, thus, limits the resolution of the sensor to 0.02 N for axial force load and to 0.003 N for the most sensitive lateral force load.

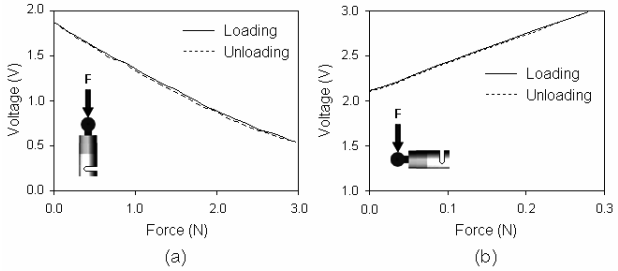

Fig. 7. (a) Responses of the sensor to axial loading and unloading, (b) Responses of the sensor that express highest sensitivity to lateral loading and unloading.

B. Tissue Tests

In order to evaluate the feasibility of using the sensor to examine soft tissues, the wheeled sensor was connected with a standard force sensor (ATI Mini40 Force/Torque Sensor) and then mounted on the distal tip of a 6 degree-of-freedom robotic manipulator (Mitsubishi RV-6SL) enabling full control of the wheeled sensor position, orientation, and movement. Before the tests were conducted, the output signal read out of the wheeled sensor was calibrated with the output of the standard force sensor. Subsequently, tissue tests were carried out in two sessions. First, *ex-vivo* static indentations were conducted with different types of tissue samples. In this case, the sensor was held vertically by the manipulator and then maneuvered down to a piece of tissue located below with a speed of 1 mm/s until it reached an indentation depth of 5 mm. Such a testing protocol was repeated with different samples of porcine organs. The responses of the sensor were recorded and plotted as shown in Fig. 8. As demonstrated in the figure, different types of organic tissues exhibited different responds due to different intrinsic viscoelastic property of the tissues. The tissue relaxations were also captured and clearly observed after the indentation had started for 5 s.

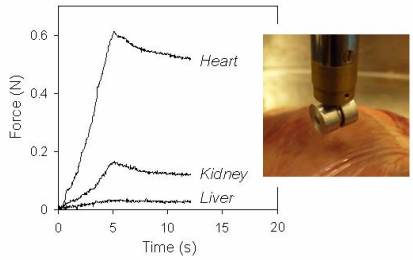

Fig. 8. Typical Responses of the porcine organs during *ex-vivo* static indentations (Note that soft tissues can exhibit a great variation of force responses depending on the indenting location, boundary conditions, pre-test conditions, and aging after death. This was clearly observed when conducting the indentation test at particular locations on the liver sample since its peak response sometimes appears to be even higher than the peak response of the kidney).

In another test session, an *ex-vivo* rolling indentation test was performed with a sample of porcine kidney which had artificially solid masses hidden underneath its surface. The objective of this test was to verify whether the sensor could be used to measure the variation of the tissue stiffness and identify the locations of artificial masses designed to simulate stiff objects such as cancerous tissues or small kidney stones. A sample of porcine kidney was prepared for the test by cutting a slice open to the boundary of the inner part (medulla) and inserting two sets of 4-mm spherical head pins at the positions that made a distance of 15 mm between each other. All pins were then covered again by the cut slice part of the kidney. To carry out the test, the sensor was initially held vertically and maneuvered down to a typical indentation depth of 7 mm. It was then moved forward with a speed of 2 mm/s allowing the wheel to roll across the kidney sur-

face which had the pins placed underneath. The same testing procedure was repeated with the kidney that had all pins removed. Fig. 9 shows the plots which represent the responses of the kidney tissue recorded by the optical sensor and the standard force sensor during a rolling indentation. As can be seen, the optical sensor records two steep peak responses from the tissue, very similar to the response from the standard force sensor. Such two steep peaks indicate the locations of the buried sets of pins—areas where the stiffness of the tissue was much higher than that of the surrounding area. This result demonstrates that the optical fiber sensor could effectively indicate the variation of the tissue stiffness and help to identify the location of buried objects and sudden variations of stiffness in an otherwise relatively homogeneous area.

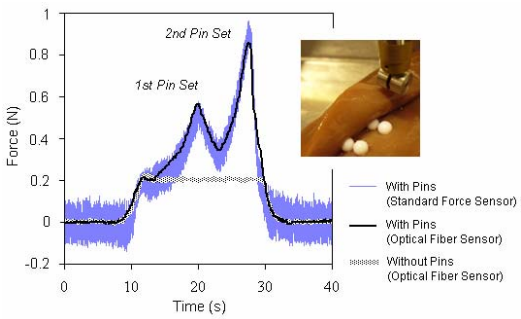

Fig. 9. Responses of the porcine kidney sample recorded by the optical fiber sensor in comparison with the signal read out of the standard sensor during an *ex vivo* rolling indentation.

IV. Discussion

Although the sensor can be used to detect the tissue interaction forces and examine variations in tissue stiffness, it cannot determine the magnitudes of the forces very accurately since the forces acting in both axial and lateral directions deform the sensing structure in a similar way. This may not be a problem if the designed sensor is applied in an application that the measured force is exerted on the sensor only in either the axial or a lateral direction. However, for the static and rolling indentation on an uneven tissue surface, the force could be generated from both directions. The sensing mechanism, which is composed of only an optical fiber pair and a single degree-of-freedom sensing structure, cannot discriminate between the effects of such force. With regard to this, an improvement of the device could be made by integrating more fiber pairs to allow multiple degree-of-freedom sensing. This will enable multi-axis force measurements to be performed. Moreover, an end stop overload protection could be introduced to protect the sensing structure from damage due to the application of excessive force. Biocompatible material such as surgical stainless steel or titanium, which is easy to clean and sterilize, should also be applied to comply with health and safety as usually required in surgery.

A major problem of adopting the optical fiber sensing methodology is due to the variation of the light signal caused by the drift of the light signal generated by the light source (LED), the bending of the fibers, and the reflectivity degradation of the reflector caused by dust particles. Since the sensor detects forces by measuring the intensity of a light signal, any changes of the light intensity other than that at the sensing mechanism will result in decreasing the effectiveness of the measurement. Without any means to prevent or compensate for such unexpected modulation of the light intensity, measurement errors could considerably degrade the sensor performance. Future work will aim at investigating these issues and further improvements on the sensor development will be carried out.

V. Conclusion

This paper reports on the design and construction of a laboratory prototype optical fiber sensor developed for detecting the mechanical responses of soft tissues during MIS. The prototype sensor was constructed to test a novel reflective intensity modulation scheme using a pair of bent-tip optical fibers to detect minute changes of the reflector edge caused by the tissue interaction forces. This sensing scenario offers very sensitive responses suitable to investigate mechanical properties of soft tissue. The sensor was successfully tested to examine a number of tissue samples. The result shows that the sensor could detect the mechanical responses of the examined samples and identify the variation of their stiffness. Such findings demonstrate the potential of the optical fiber sensors integrated with equipment that helps the surgeons to perform soft tissue examination during minimally invasive surgical procedures.

References

[1] J. Peirs, J. Clijnen, D. Reynaerts, H. Van Brussel, P. Herijgers, B. Corteville, and S. Boone, "A micro optical force sensor for force feedback during minimally invasive robotic surgery", *Sens. Actuators A*, vol. 115, pp. 447-455, Sept. 2004.

[2] U. Seibold, B. Kuebler, and G. Hirzinger, "Prototype of instrument for minimally invasive surgery with 6-axis force sensing capability", in *Proc. IEEE Int. Conf. Robot. Autom.*, 2005, pp. 496-501.

[3] P. Valdastri, K. Harada, A. Menciassi, L. Beccai, C. Stefanini, M. Fujie, and P. Dario, "Integration of a miniaturised triaxial force sensor in a minimally invasive surgical tool", *IEEE Trans. Biomed. Eng.*, vol. 53, pp. 2397-2400, Nov. 2006.

[4] K. Tadano, and K. Kawashima, "Development of 4-DOFs forceps with force sensing using pneumatic servo system", in *Proc. IEEE Int. Conf. Robot. Autom.*, 2006, pp. 2250-2255.

[5] D. Noonan, H. Liu, Y. H. Zweiri, A. A. Althoefer, and L. D. Seneviratne, "A dual-function wheeled probe for tissue viscoelastic property identification during minimally invasive surgery", in *Proc. IEEE Int. Conf. Robot. Autom.*, 2007, pp. 2629-2634.

[6] A. Bicchi, G. Canepa, D. De Rossi, P. Iacconi, and E. P. Scilingo, "A sensorized minimally invasive surgery tool for detecting tissutal elastic properties", in *Proc. IEEE Int. Conf. IEEE Robot. Autom.*, 1996, pp. 884-888.

[7] S. Hirose, and K. Yoneda, "Development of optical 6-axial force sensor and its signal calibration considering non-linear interference", in *Proc. IEEE Int. Conf. Robot. Autom.*, 1990, pp. 46-53.

[8] M. Lazeroms, G. Villavicencio, W. Jongkind, and G. Honderd, "Optical fibre force sensor for minimal-invasive-surgery grasping instruments", in *Proc. IEEE Eng. Medicine Biol. Soc. Int. Conf.*, 1996, pp. 234-235.